Green Chemistry

PAPER

View Article Online
View Journal | View Issue

CrossMark click for updates

Cite this: *Green Chem.*, 2016, **18**, 6516

Supercritical water hydrolysis: a green pathway for producing low-molecular-weight cellulose†

Jean Buffiere,[a] Patrik Ahvenainen,[b] Marc Borrega,[a] Kirsi Svedström[b] and Herbert Sixta*[a]

Received 10th September 2016,
Accepted 19th September 2016

DOI: 10.1039/c6gc02544g

www.rsc.org/greenchem

This work discusses the suitability of supercritical water treatment (SCWT) for depolymerising microcrystalline cellulose in a controlled way. The SCWT partially hydrolysed cellulose down to a mixture of three valuable products: water-insoluble low-molecular-weight cellulose (WI-LMWC) precipitate, water-soluble low-molecular-weight cellulose (WS-LMWC) oligomers, and glucose. The conditions under which the energy demand for obtaining these products is minimised were identified by adjusting the reaction time inside the continuous reactor and the temperature around the critical point. The optimum conditions were 370 °C and 0.4 seconds for producing WI-LMWC and 360 °C and 0.5 seconds for producing WS-LMWC, with maximum yields of 19 wt% and 50 wt%, respectively. This work also shows that the water-insoluble product precipitates into crystalline cellulose II arrangements. This precipitation phenomenon enabled isolation of cellulose chains of different lengths according to their respective solubilities in ambient water. The results show that SCWT is a relevant process for producing narrowly distributed fractions of low-molecular-weight cellulose using water and heat only.

1. Introduction

Cellulose, with an estimated natural production above one trillion tons annually, is the most abundant bio-based polymer on Earth.[1] Found mainly in plant biomass, cellulose can today be used in a wide range of applications, from paper to transparent films, and from textile fibres to absorbing materials. It is also a major source of glucose in lignocellulosic plants; for this reason, cellulose is currently investigated as a renewable, non-food raw material for producing various glucose-derived chemicals, such as ethanol,[2] levulinic acid,[3] and furfural.[4] As the main component in the plant cell wall, cellulose is a resistant yet flexible material whose properties are due to its unique composition. Structurally, it is a linear polymer with long chains of repeating anhydroglucose units (AGUs) linked to each other by glycosidic bonds. The length of the cellulose chains is an important parameter when designing cellulose-based materials. In its native form, its degree of polymerisation (DP) can be as high as 5000 AGUs for some plant species.[5] However, most uses of cellulose require its preliminary isolation and purification from the other biomass components, using mechanical and chemical treatments that significantly decrease the DP depending on their intensities.[6]

The individual cellulose chains are tightly bound together into semi-crystalline arrangements *via* an extensive network of hydrogen interactions,[7] which provide both mechanical strength and flexibility to the plants.[8] These arrangements are commonly modelled as two-phase systems composed of crystalline regions, the crystallites, as well as amorphous regions linking the crystallites together. The crystallites are densely packed structures and thus are more resistant to depolymerisation than the less crystalline fractions, which can easily be hydrolysed using mineral acids or enzymes. The residue of the mild acid hydrolysis of cellulose is highly crystalline and its DP reaches a constant level after a certain treatment time, which is commonly referred to as the levelling-off degree of polymerisation (LODP).[9] The resulting microcrystalline cellulose (MCC) is commercially used in various applications, including as a bulking agent in drugs and foods.

The hydrolysis of MCC below the LODP is generally a more demanding process due to the limited accessibility of the glycosidic bonds within the crystallites. Because supercritical water has the ability to dissolve crystalline cellulose structures and to depolymerise them, the supercritical water treatment (SCWT) of cellulose has been proposed as an alternative method to acid-catalysed hydrolysis.[10] Supercritical water refers to pure water heated and pressurised above its critical point (374 °C and 22.1 MPa). Towards the critical point, several of the main properties of water, such as density,

[a]*Department of Forest Products Technology, School of Chemical Technology, Aalto University, P.O. Box 16300, 00076 Aalto, Finland. E-mail: herbert.sixta@aalto.fi*
[b]*Department of Physics, University of Helsinki, P.O. Box 64, 00014 Helsinki, Finland*
†Electronic supplementary information (ESI) available. See DOI: 10.1039/c6gc02544g

viscosity, and dielectric constant gradually decrease with increasing temperature.[11] Above the critical point, all these properties further undergo a sharp decrease. In contrast, at 25 MPa the ionic product of water reaches a maximum around 260 °C of approximately 10^{-11}, then decreases to reach values as low as $10^{-16.5}$ at 400 °C.[12] These conditions trigger the rapid cleavage of glycosidic bonds, the dissolution of the hydrolysed cellulose chains, and can fully degrade an MCC suspension into water-soluble products within a second.[13]

Supercritical reactors usually operate at a fixed pressure of 25 to 30 MPa while temperature and treatment time are the two main variables of the reaction. The degradation of MCC in nearcritical and supercritical water is best described by the shrinking core model.[10,14] In addition, an Arrhenius plot of the kinetic constants usually exhibits a significant increase in the MCC conversion rate around the critical point.[15] Unlike with conventional acid-catalysed hydrolysis at low temperatures, the cellulose chains are extensively swollen or dissolved under nearcritical and supercritical water conditions, which significantly enhances their accessibility.[14,16] This enables homogeneous hydrolysis to take place, where the chains are randomly cleaved along the polymer length.[17] Thus, cellulose is first hydrolysed into low-molecular-weight chains, which are then further hydrolysed to glucose.

Hydrolysis is, however, not the only reaction taking place during SCWT. Glucose and cellulose oligomers are further degraded into non-cellulosic products through parallel retro-aldol condensation, fragmentation, and dehydration reactions that compete with hydrolysis and reduce the overall selectivity of the process.[18,19] The main products of these side reactions have been identified in the literature as a complex mixture of fructose, levoglucosan, erythrose, glycolaldehyde, 5-hydroxymethylfurfural, as well as other water-soluble organic compounds.[17,20] These reactions can be minimised by using high temperatures and extremely low reaction times: by decreasing the duration of the reaction down to a few hundredths of a second at 400 °C, a promising selectivity as high as 98% could be reached.[19] Such high selectivity levels could enable the upscaling of SCWT plants for producing cellulosic glucose, provided that such low reaction times can be maintained on larger scales.

Supercritical water is, however, not only a promising and environmentally friendly medium for producing cellulosic glucose but, in the random fashion in which the glycosidic bonds are cleaved, is also suitable for producing cellulose oligomers, commonly referred to as cello-oligosaccharides or cellodextrins.[17] However, the industry currently lacks an industrial method to produce cello-oligosaccharides.[21] Currently known production pathways either involve partial hydrolysis using mineral acids,[22] acetolysis followed by deacetylation,[23] long-time treatment in concentrated phosphoric acid and subsequent fractionation,[24] the combination of ball-milling and plasma treatment,[25] or complex synthesis routes.[26] In this regard, SCWT can be a solid alternative to the existing pathways for partially depolymerising cellulose as well as for producing low-molecular-weight cellulose (LMWC), thereby closing the existing DP availability gap between the short-chain oligomers and MCC.[24]

LMWC is extensively formed as an intermediate compound during supercritical water hydrolysis. The chains are dissolved in nearcritical and supercritical water but the oligomers with a DP above 6 have very limited solubility in ambient water; this difference causes the longer cello-oligosaccharides, or water-insoluble low-molecular-weight cellulose (WI-LMWC), to slowly precipitate after the reaction.[27] The precipitated material is known to be composed of cellulose II, which indicates that nearcritical and supercritical conditions can swell or fully dissolve LMWC.[28] In contrast, the shorter cello-oligosaccharides have a higher solubility in ambient water: they are referred to as water-soluble low-molecular-weight cellulose (WS-LMWC) as they remain dissolved in solution after the reaction.

These two products contain valuable compounds that are potentially suitable in both analytical and industrial applications, either as mixtures or after separation as individual oligomers. The mixtures of WS-LMWC oligomers could be used as food additives for their assumed prebiotic properties and positive effects on health, as recently found using cello-oligosaccharides produced by many conventional pathways.[29,30] In addition, the WI-LMWC fraction could be used as a direct compression excipient in fast-release drugs, as LMW cellulose II powders have already shown improved properties in such applications compared to those formulated using conventional MCC.[31,32]

Nevertheless, using supercritical water to hydrolyse cellulose remains a recent approach and its potential beyond that of scientific curiosity remains unclear even today. The present research depicts a practical approach to partially depolymerise MCC using nearcritical and supercritical water to produce both WS-LMWC and WI-LMWC. The experiments aim at identifying the effect of reaction conditions such as treatment time and temperature on the degradation of MCC and on the formation of LMWC. The effect of the SCWT on the structural and macromolecular properties of the cellulosic products is also investigated. Furthermore, the heat demand associated with the use of supercritical water is assessed as a method to identify the best experimental conditions for producing either WS-LMWC or WI-LMWC. Finally, a method for narrowing the DP distribution of the precipitated fraction is presented, thereby making LMWC with distinct DP ranges available for further use.

2. Experimental

2.1. Supercritical water treatment

The SCWT was performed using a plug-flow reactor, whose concept and operation principles have already been described in previous work.[16] MCC was purchased from Merck (Darmstadt, Germany; Ref. 1.02330.0500) and was used as received. A 1.0 wt% MCC suspension was pressurised and mixed with a preheated supercritical water stream with a ratio of 2 : 3 at the one end of a tubular reactor (diameter 3 mm,

length 55 mm). The reaction was stopped by quenching with a cold water flow at the other end of the reactor down to a sub-critical temperature of 268 °C, after which the product was further cooled down using a cold water jacket and depressurised to atmospheric pressure for sample collection. All reactor streams used deionised water. The correct reaction time for each experimental point was achieved by individually setting the mass flow rates entering the reactor. In addition, the temperature after quenching was kept constant throughout the experiments by adjusting the quenching flow rate. Furthermore, external heating elements placed around the reactor compensated for the heat losses; therefore, the reactor was considered isothermal.

The treatment of MCC was performed at four different temperatures around the critical point (360 °C, 370 °C, 380 °C and 387 °C, the latter being the highest temperature achievable using this experimental setup) and at various reaction times (0.1 to 0.6 s). The pressure was held constant at 25 MPa. The lowest treatment time (0.1 s) could only be reached at 380 C and 387 °C due to the lower water density at these temperatures. Under each of these conditions, 40 ml samples were collected in duplicate and fractionated according to the procedure described in the following paragraph. Table 1 summarises the experimental conditions as well as the main properties of water at the corresponding treatment temperatures.

Immediately after production, the residual suspended solids were separated either by ultracentrifugation (Eppendorf model 5804 R, Hamburg, Germany) at 10 000 rpm for 30 min or by filtration over a 0.45 μm syringe filter with the GHP membrane (Pall, New-York, USA). Next, the samples were allowed to settle at 5 °C for seven days, during which a white solid precipitate appeared in most samples. The precipitated material, referred to as WI-LMWC in the next section, was separated by filtration and centrifugation using the same procedure as for the residual fraction; therefore, two distinct solid products were isolated: the residue and the WI-LMWC precipitate. The two separation steps left a clear, stable liquid fraction composed of WS-LMWC oligomers, glucose, and non-cellulosic degradation products. The three products (residue, precipitate and liquid fraction) were analysed according to the methods described in the following section.

2.2. Analytical methods

The yield of the two isolated solid fractions, namely the residue and the precipitate, was quantified gravimetrically by weighing the 0.45 μm syringe filters before and after filtration, in both cases after drying overnight at 105 °C. In addition, the molecular weight distribution (MWD) of cellulose in these two fractions was characterised upon centrifugation using size-exclusion chromatography (SEC). SEC was performed in DMAc/LiCl 9 g l^{-1} using a Dionex (Sunnyvale, USA) Ultimate 3000 system, one guard and four analytical Agilent (Santa Clara, USA) PL-gel Mixed-A columns, coupled with a Shodex (Tokyo, Japan) RI-101 refractive index detector. The samples for SEC underwent a preliminary procedure in order to enhance their solubility in the DMAc/LiCl solvent system: they were successively activated in water, in acetone, and in DMAc. The samples were finally dissolved in saturated DMAc/LiCl 90 g l^{-1}, diluted with pure DMAc down to a sample concentration of 1.0 mg ml^{-1} and a final LiCl concentration of 9 g l^{-1}, and filtered through a 0.2 μm GHP syringe membrane filter into a vial for analysis. Each sample was analysed in duplicate, with two injections of 100 μl each. The resulting distributions were calibrated using a set of eleven pullulan standards (PSS, Mainz, Germany) with molecular weights ranging from 342 Da to 2350 kDa.

Wide-angle X-ray scattering (WAXS) was used in perpendicular transmission mode to study the solid fractions. Copper Kα energy (8.0 keV) was used with the two-dimensional detector set-up described in a previous paper.[33] The powders were hand-pressed into 0.9 mm thick metal rings that were sealed with Mylar foils. The WAXS data were corrected for read-out noise of the detector and normalised with the primary beam transmission before Mylar and air background subtraction. After this, polarisation, flat panel, and irradiated volume corrections were applied to the data.

The degree of crystallinity was determined by using a modified version of the amorphous fitting method.[34] Diffraction peaks of both cellulose $I\beta^7$ (n = 18) and cellulose II^{35} (n = 17) were fitted to the radial integrals along with the amorphous model (sulphate lignin). To reduce the number of free fitting parameters, the positions of the cellulose II peaks were fixed to those obtained from the WI-LMWC and the relative height

Table 1 Experimental conditions used in this study and water properties at the corresponding temperatures. A cross represents an experimental point

	Temperature	360 °C	370 °C	380 °C	387 °C
Reaction time	0.1 s			X	X
	0.2 s	X	X	X	X
	0.3 s	X	X	X	X
	0.4 s	X	X	X	X
	0.5 s	X	X	X	X
	0.6 s	X	X	X	X
Water properties (25 MPa)	Density (kg m^{-3})	589.3	540.5	450.8	254.6
	Ionic product (−)	$10^{-11.74}$	$10^{-12.03}$	$10^{-12.69}$	$10^{-14.89}$
	Dielectric constant (−)	12.6	10.2	7.8	6.3
	Specific enthalpy (kJ kg^{-1})	1698.6	1789.8	1935.7	2286.4

and the peak width were limited to be within 5% of the corresponding values of the precipitate. One fitting parameter was used as a coefficient for all the cellulose II peak heights in order to adjust the relative cellulose II content. The final cellulose II content was calculated as the relative area of the cellulose II component relative to the entire crystalline cellulose fit area (cellulose I and cellulose II). The crystallinity value calculated describes the total crystalline content in the sample. Both crystallinity and cellulose II content were determined from the scattering angle region between 10 and 42 degrees.

The average crystallite size was estimated with the Scherrer formula[36] based on the widths of the diffraction peaks. For assessing the dimensions of the crystallites, the limits mentioned above for cellulose II parameters were optimised to obtain an optimal fit for the diffraction peaks used and, thus, reliable diffraction peak widths. The crystallite size was determined for reflections for which the corresponding peak width could be estimated.

For the liquid fraction, total organic carbon (TOC) measurements with Shimadzu (Kyoto, Japan) TOC-V CPH apparatus gave an estimate of the total dissolved carbon in each sample. Assuming negligible gas formation during the SCWT and thus an unchanged average molecular weight in the product fraction of 162 g mol^{-1}, TOC allowed quantification of the total dissolved solids in the samples. In addition, the share of dissolved glucose and cello-oligosaccharides in the liquid fraction was quantified by high performance anion-exchange chromatography with pulsed amperometric detection (HPAEC-PAD) using a Dionex ICS-3000 apparatus equipped with a CarboPac PA100 column. Calibration curves were obtained from standard glucose and cello-oligomer compounds with DP 2 to 6 from Megazyme (Wicklow, Ireland) using solutions with concentrations ranging from 2 to 50 mg l^{-1}, which were then extrapolated to DP up to 10 according to the height of the corresponding amperometric signals. Importantly, repeated calibration trials showed significant variability in the HPAEC-PAD calibration. The most conservative calibration values were selected; therefore, real amounts of glucose and water-soluble oligomers in the samples might be slightly higher than the values presented in the following sections.

3. Results and discussion

3.1. Product mass balance

MCC was rapidly degraded when subjected to nearcritical or supercritical water treatment. The full conversion of MCC, as defined by the ratio between the concentration of residual cellulose and the initial MCC concentration, was achieved within 0.5 seconds at all temperatures, which is in good accordance with previously published work.[16] After fractionation and analytical characterisation, the mass balance of the product samples contained five components, two of which were solid: the undissolved residue and the WI-LMWC precipitate. The remaining liquid fraction contained WS-LMWC oligomers, glucose, and non-cellulosic compounds. The chemical composition, mechanism of formation and yield of these non-cellulosic compounds were extensively investigated in the literature, including a recent study using the same experimental setup.[17] Therefore, analysing these compounds was voluntarily left out of the scope of the present research; they are referred to as a single category of products.

Two observations can be drawn from the mass balance regarding the effect of temperature and reaction time on the kinetics and mechanism of MCC conversion in nearcritical and supercritical water, shown in Fig. 1. First, the higher the temperature and the longer the treatment time, the more cellulose was converted. The yield of glucose and non-cellulosic products generally increased with the duration of the reaction, while the amount of WS-LMWC oligomers and the WI-LMWC precipitate only increased until full MCC conversion was achieved. In addition, the WI-LMWC was found only at low-to-intermediate reaction times, reaching a maximum after 0.3 s to 0.5 s depending on the temperature. The yield of WI-LMWC reached a maximum at 370 °C for a reaction time of 0.4 seconds, accounting for up to 18.7% of the product fraction.

The hypothesis of a random hydrolysis mechanism where LMWC is formed as an intermediate either as WI-LMWC or as WS-LMWC seemed to apply well in both nearcritical and supercritical water. In addition, the increase in the quantity of non-cellulosic products formed with increasing reaction time and temperature validates the proposed degradation mechanism that involves a series of consecutive hydrolysis steps occurring in parallel with competing, non-hydrolysis reactions.

The degradation of cellulose visibly occurred faster at higher temperatures, as previously described in the literature.[14,37] However, the products formed were comparable in terms of yields at all temperatures, which indicates that despite an increase in the kinetic rates the overall degradation mechanism remained the same across the temperature range investigated. Only at the highest temperature of 387 °C and above a reaction time of 0.4 s did cellulose undergo a near-complete hydrolysis, with no WI-LMWC formed and decreasing amounts of WS-LMWC. However, the near-complete hydrolysis was not accompanied by significantly higher glucose yields, which confirms the importance of parallel, non-hydrolysis reactions in the degradation mechanism even at supercritical temperatures.

3.2. Liquid fraction and WS-LMWC

The mass balance introduced in the previous section indicated that glucose and WS-LMWC oligomers accounted for a significant share of the products under all conditions. The concentration of dissolved glucose and individual cello-oligosaccharides is shown as a function of reaction time and treatment temperature in Fig. 2. The curves obtained from HPAEC-PAD confirm the extensive formation of LMWC during SCWT. The presence of a mixture of glucose and cellulose oligomers of various lengths confirms the hypothesis of a random cleavage of the glycosidic bonds in the chains, as predicted by the Flory-Schulz model fitted on the overall product distribution obtained under similar experimental

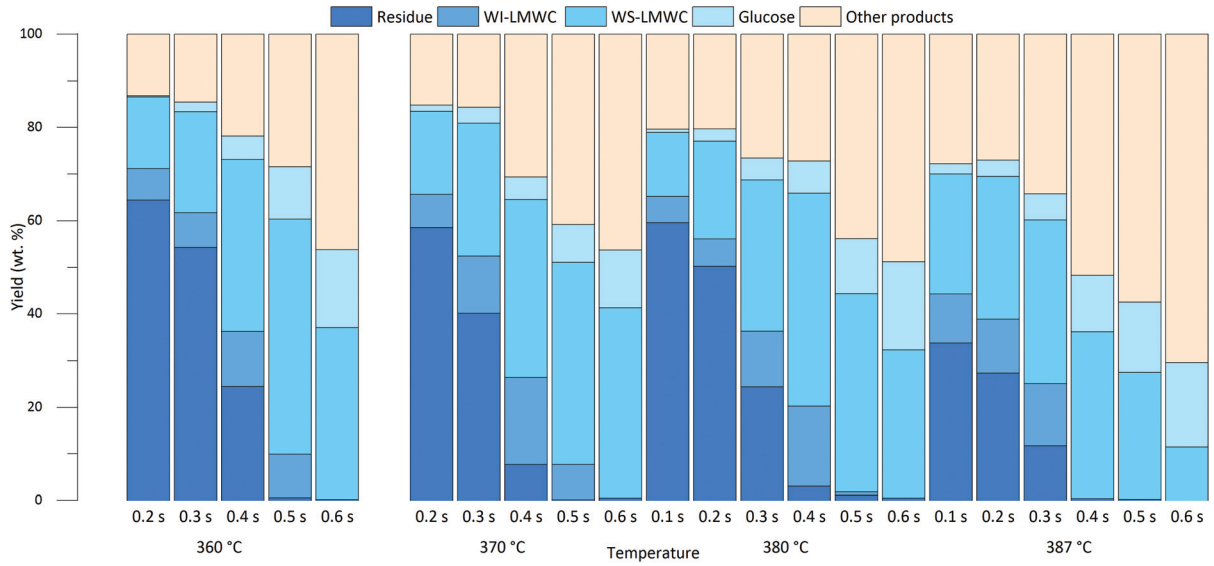

Fig. 1 Yields of the five product fractions as a function of reaction time at various treatment temperatures.

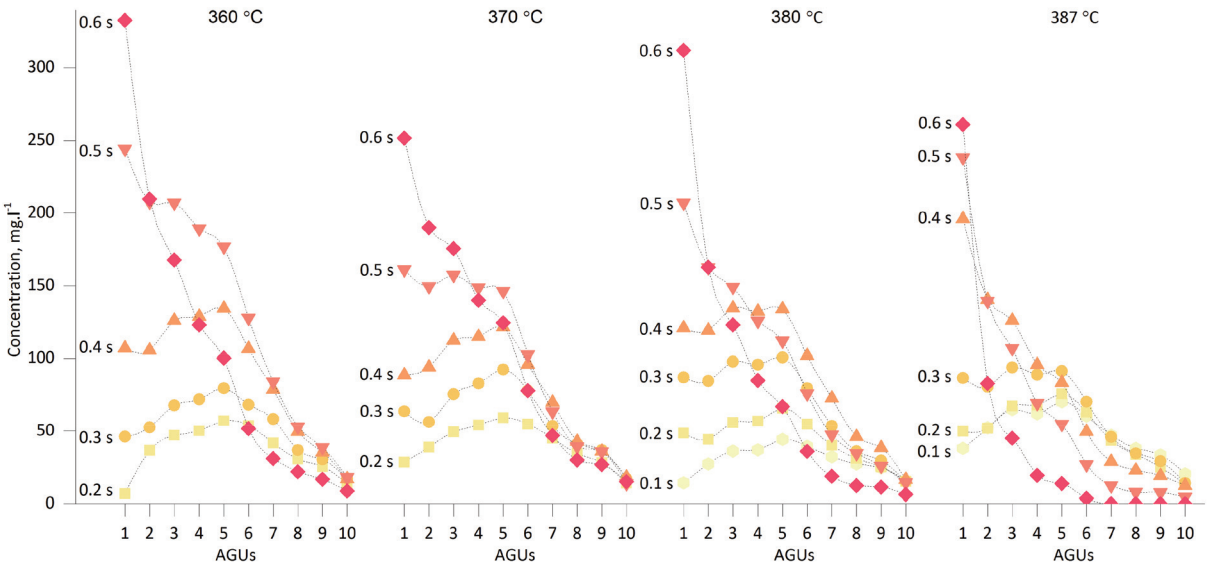

Fig. 2 Evolution of dissolved glucose and cello-oligosaccharide concentration as a function of reaction time at various treatment temperatures.

conditions.[17] The random scission model appears to be a more valid hypothesis than Sharples's endwise depolymerisation model generally observed in acid-catalysed hydrolysis of crystalline cellulose,[38] which would result in significantly higher glucose-to-oligomer ratios than those in the present case, as confirmed by computer simulation that predicted the final molecular weight distribution based on different modes of chain scission.[39]

The amounts of dissolved cello-oligosaccharides increased with reaction time at all temperatures, except for the two longest reaction times of 0.6 s and especially for temperatures above the critical point. At 387 °C and 0.6 s only DPs below 6 were present, confirming a near-complete cellulose hydrolysis.

In addition, the concentration of dissolved oligomers with a DP between 6 and 10 AGUs was relatively low and decreased with increasing DP; this phenomenon was visible under all experimental conditions. This confirms the limited solubility of cello-oligosaccharides in ambient water as previously predicted by Gray *et al.* in a dedicated study.[40] According to Fig. 2 the maximum concentration of these oligomers was similar across the temperature range; this might indicate that the solubility limit for these oligomers was reached.

The highest concentrations of water-soluble cello-oligosaccharides were reached at nearcritical temperatures. The largest share of the WS-LMWC fraction was obtained at 360 °C and 0.5 s, and accounted for 50% of the total mass balance

presented in Fig. 1. In addition, these conditions showed the lowest formation of non-cellulosic products once full cellulose conversion was reached, making them all more relevant for obtaining cello-oligosaccharides as the final product.

3.3. Solid fractions and WI-LMWC

While the previous section focused on the formation of glucose and WS-LMWC under nearcritical and supercritical conditions, this section focuses on the effect of SCWT on the DP of the two isolated solid products: the residue and the WI-LMWC precipitate. Fig. 3 shows the effect of nearcritical and supercritical water treatments on the weight-average degree of polymerisation (DP_w) and the polydispersity index (PDI) of these two fractions, as obtained by SEC. Fig. 3a shows that the residual cellulose underwent a major reduction in its DP_w already at lower reaction times, compared to that of the initial MCC. Increasing the duration of the treatment resulted in a further and progressive reduction, albeit limited compared to the initial depolymerisation. In addition, for a given reaction time the reduction was more pronounced with increasing temperature. Importantly, most residue samples had a DP_w between 50 and 150 AGUs, which is lower than that of any of the commercially available celluloses.[24]

In contrast, the WI-LMWC precipitate showed surprisingly low DP_w with an average value of around 20 AGUs across the samples, as depicted in Fig. 3b. In addition, the DP_w of the precipitate samples was independent of the temperature and time variables used to produce them, which indicates that the ability of water to dissolve LMWC remained practically the same throughout the investigated temperature range. The stability of the DP_w of the WI-LMWC precipitate obtained under various conditions is comparable with the early observations made by Sasaki *et al.*[28]

As far as the polydispersity is concerned, the SCWT did not result in a significant reduction in the PDI of the residue despite the drop in DP_w previously observed, except that after longer reaction times. At no point did the residue reach a PDI value below 2. In contrast, unlike the residue, the WI-LMWC exhibited very low PDI, with an average of 1.5, as shown in Fig. 3d. This observation confirms the hypothesis of a substantial increase in the LMWC solubility range under nearcritical and supercritical water conditions compared with ambient conditions. The LMWC chains are instantaneously dissolved upon hydrolysis during the treatment. The differential solubility then causes the chains with a DP_w of around 20 to slowly precipitate, while the oligomers up to DP 6 retain a significant solubility in ambient water, as previously observed in Fig. 2. Indeed, it has been observed that oligomers with a DP above 6 retain a very low solubility in water once precipitation is complete.[27] Therefore, the phenomenon enables isolation of a narrowly distributed, WI-LMWC fraction from an initially much wider cellulose distribution.

Investigating the structure of the solid products using WAXS provided additional indications concerning the physical mechanisms involved during SCWT. The scattering intensities of the initial MCC as well as the residue and precipitate fractions obtained at 370 °C and 0.4 s are shown in Fig. 4. The numerical data for the crystallinity, the size of the crystallites as well as the cellulose II content are summarised in Table 2. The data clearly indicate that while MCC only contained native cellulose I allomorph, the WI-LMWC was almost entirely composed of the cellulose II allomorph typical of swollen or dissolved cellulose. This confirms the fact that the WI-LMWC

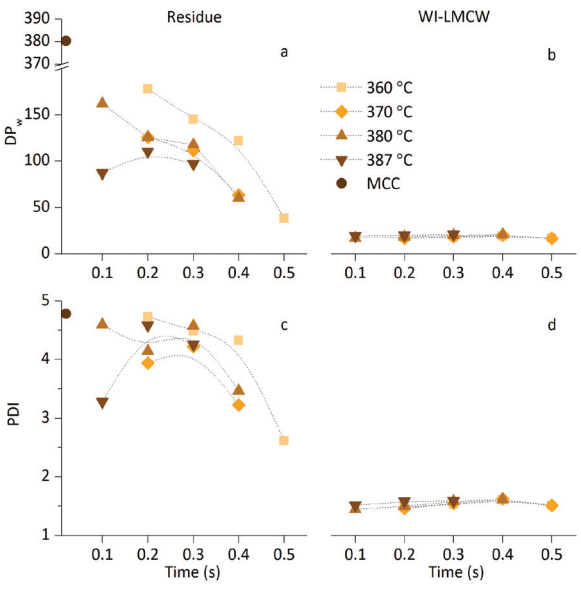

Fig. 3 Effect of treatment on the cellulose in the solid fractions. Top: Weight-average degree of polymerization (DPw) of a. residue and b. WI-LMWC. Bottom: Polydispersity indices (PDI) of c. residue and d. WI-LMWC.

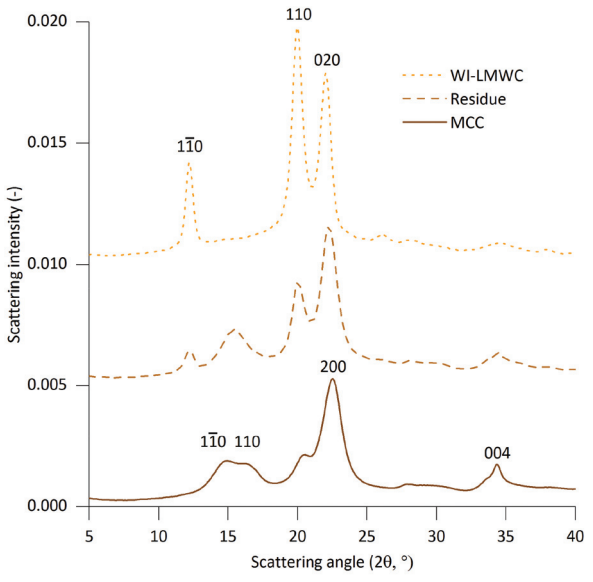

Fig. 4 WAXS intensities of MCC and the two isolated product fractions obtained at 25 MPa, 370 °C and 0.4 s: residue and WI-LMWC. Intensities are shifted vertically for clarity.

Table 2 WAXS data for MCC and two solid product fractions obtained at 25 MPa, 370 °C and 0.4 s: residue and WI-LMWC. Annotations: [I]Cellulose I, [II]Cellulose II, *(±1.0 nm), **(±0.5 nm), ***(±0.3 nm), ~(±5%), ~~(±3%)

			Crystallite size		
			Reflection		
	Cellulose II content	Crystallinity	$1\bar{1}0$	110	200
MCC	0%~	51%~~	4.2 nm^{I**}	5.6 nm^{I**}	5.0 nm^{I***}
Residue	37%~	55%~~	9.5 nm^{II*}	10.2 nm^{II*}	—
WI-LMWC	94%~	55%~~	11.8 nm^{II*}	11.2 nm^{II*}	—

precipitated from an initially dissolved state after SCWT. In addition, the residue fraction contained both cellulose I and cellulose II, thus indicating a mixture of native and regenerated cellulose. A closer look at the MWD of the undissolved residue, shown in Fig. 5, revealed a two-phase compound composed of a low-molecular-weight fraction similar to that of the pure WI-LMWC but having a higher molecular weight, as well as a high-molecular-weight shoulder with significantly shorter chains than that in the high-molecular-weight region of the initial MCC. The low-molecular-weight region could correspond to the cellulose II chains. This LMWC might have precipitated right after the treatment before the separation of the residue, thus explaining the coexistence of cellulose I and II within the same sample.

The relatively high peak areas revealed a high level of crystallinity of above 50% for all samples. The SCWT had little influence on the cellulose crystallinity. The average size of the crystallites was significantly higher for the precipitated WI-LMWC than that for the MCC, while the value for the residue was in between these. These results are in accordance with the observations made from cellulose samples after treatment in subcritical water, where an increase in the crystallite size was observed with increasing cellulose conversion for the 110 and 200 reflections.[33] In addition, a qualitative change was observed between the MCC and the residue in the WAXS intensities in the scattering angles corresponding to the cellulose Iβ $1\bar{1}0$ and 110 diffraction peaks. As there are no significant cellulose II peaks in this scattering angle range, the change is due to a change in the cellulose I structure. The crystalline structure similar to the one present in the residue is sometimes referred to as cellulose IV_I, although it is more recently considered to be cellulose Iβ with lateral disorder or a unique crystallite shape.[41] A similar structure has been observed in previous subcritical and supercritical water treatments of cellulose I.[16] The cellulose Iβ 004 diffraction peak was also broader in the residue compared to that of MCC, suggesting a decreased crystallite length, which correlates with the decrease in DP_w observed in Fig. 3. However, due to its broadness and the overlap with other diffraction peaks, no quantitative assessment of the average crystallite length could be made from the 004 peak.

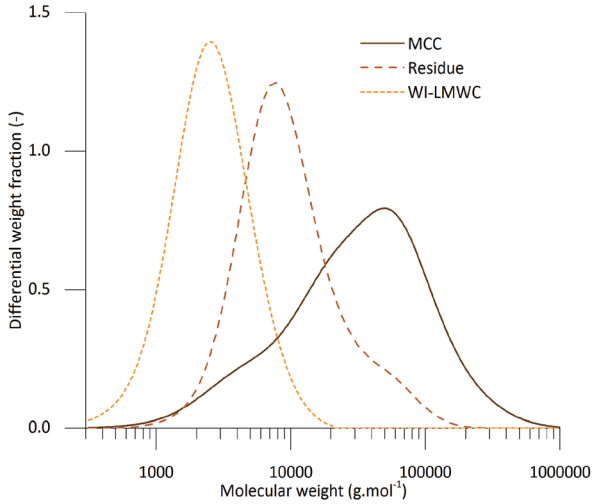

Fig. 5 Molecular weight distributions (MWDs) of MCC and the two solid fractions obtained at 25 MPa, 370 °C and 0.4 s: residue and WI-LMWC.

3.4. Optimal reaction conditions

The data presented in the previous two sections confirmed that both the temperature and the residence time inside the reactor are crucial parameters for the SCWT. These two variables determine the yield of WI-LMWC and WS-LMWC fractions as well as the overall extent of cellulose depolymerisation. In addition, the two parameters determine the temperature and flow rate of the preheated supercritical water stream needed to bring the cellulose suspension to nearcritical or supercritical conditions and thus the overall energy demand for the process. Unlike conventional hydrolysis methods requiring mineral acids or enzymes, the energy input needed in the SCWT is significant; optimal conditions must be found, that can minimise the energy demand.

Regarding the energy balance, increasing the treatment temperature has two competing effects, as shown in Fig. 6. On the one hand, the water density decreases, which allows reaching the same reaction times using lower mass flow rates. On the other hand, the specific enthalpy of water increases, which raises the amount of energy needed to heat up a given mass flow. This energy demand d (kJ g^{-1}) can be calculated relative to the experimental concentration of the desired product w (g g^{-1}). Eqn (1) shows such a calculation using the actual mass flow rates of the supercritical water stream q_{scw}, of the cellulose suspension stream q_{MCC}, and of the quenching water

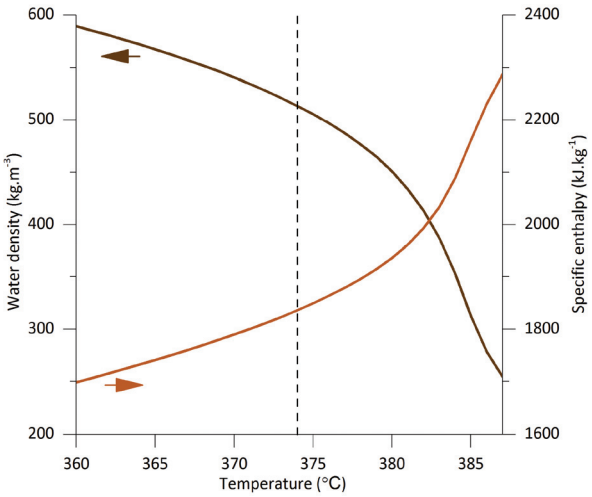

Fig. 6 Density and specific enthalpy of water at 25 MPa around the critical point, represented by a vertical dashed line. The arrows show which *y* axis corresponds to the curve. Adapted from Lemmon *et al.*[11]

stream q_{qw} (g s^{-1}), as well as the specific enthalpy needed to heat up the supercritical water stream. The specific enthalpy is obtained as the difference between that of the preheated water in the supercritical water stream and that of the water at the initial temperature and pressure of 20 °C and 0.1 MPa $h_{scw} - h_{20°C,\ 0.1Mpa}$ (kJ g^{-1}).

$$d = \frac{q_{scw} \times (h_{scw} - h_{20°C,\,0.1Mpa})}{w \times (q_{MCC} + q_{scw} + q_{qw})} \quad (1)$$

Fig. 7a, b and c depict the energy demand for producing the three main products of the SCWT: the WI-LMWC precipitate, a mixture of WS-LMWC oligomers, and glucose, respectively. The graphs indicate that the operating conditions have a major impact on the energy demand for producing three compounds, although the trends remain generally similar across the temperature range. The influence of temperature is unclear in the case of WI-LMWC despite the fact that the corresponding energy demand is the lowest at 0.4 seconds at three temperatures, reaching a minimum at 370 °C and 0.4 seconds. In addition, the energy demand is minimised for WI-LMWC at 360 °C and 0.5 seconds. In contrast, the energy demand for producing WS-LMWC slowly decreases with increasing reaction time up to 0.5 seconds, except that at 387 °C where the demand drastically increases after long reaction times. This is a result of cellulose reaching near-complete conversion under these conditions, as observed in Fig. 2. In addition, the corresponding minimum energy needed is 3250 kJ g^{-1} for WI-LMWC and 1020 kJ g^{-1} for WS-LMWC. These two products are intermediates in the hydrolysis and are both composed of LMWC with various chain lengths while glucose is the single product of complete cellulose depolymerisation and thus requires longer reaction times to be formed, as indicated by a decreasing energy demand with increasing reaction time at all temperatures. The energy demand for producing glucose reaches a minimum of 3380 kJ g^{-1} after a treatment of 0.6 seconds at 360 °C.

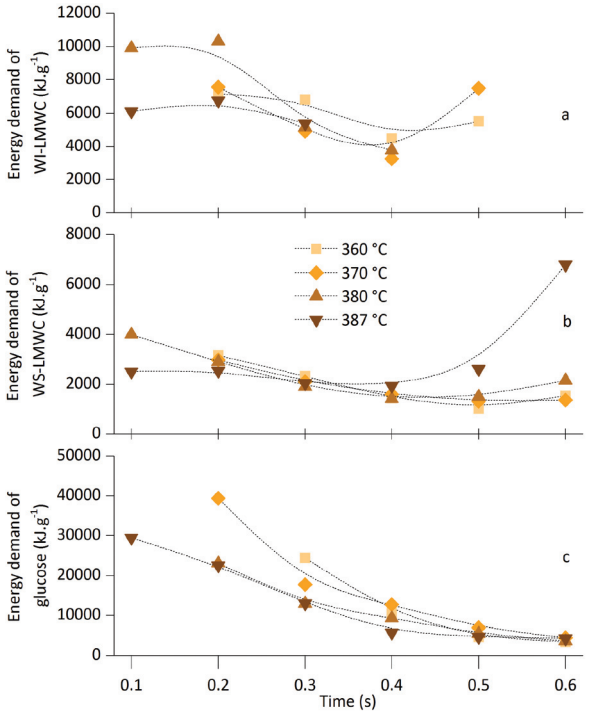

Fig. 7 Energy demand for producing a. WI-LMWC, b. WS-LMWC, and c. glucose as a function of reaction time and at various treatment temperatures. The demand is expressed in kJ needed to heat up the supercritical water stream per gram of product obtained.

While there is no doubt that the energy input can be easily and significantly reduced by implementing a heat recovery strategy for the process, the cost of cellulose cannot be neglected because of the limited yields of the three products: 18.7% for WI-LMWC, 50.8% for WS-LMWC, and 19.1% for glucose. Reaching high yields and selectivity towards cellulose hydrolysis and towards the formation of the desired products is critical. Regarding the yields it was shown that the quantity of WI-LMWC and WS-LMWC formed is highly dependent on the reactivity of the raw material; various MCCs gave very different yields.[13] For commercial MCC, the mass balance presented in Fig. 2 indicated that both maximum selectivity and maximum share of glucose, WS-LMWC and WI-LMWC are reached slightly below full MCC conversion. In addition, in this study lower temperatures generally resulted in slightly higher selectivity for a given level of MCC conversion.

3.5. Low-molecular-weight celluloses

As described in the previous sections, the high energy demand, temperature and pressure levels as well as low reaction times required do not make the SCWT an easy hydrolysis process to be implemented industrially at the moment. However, this unique method in which supercritical water simultaneously hydrolyses and dissolves cellulose chains can be used to easily obtain narrowly distributed LWMC fractions. In

addition to the initial WI-LMWC, the decrease in solubility with increasing oligomer DP enables isolation of cellulose fractions with DP_w distributions slightly narrower than the initial precipitated fraction. This can be achieved by two methods: by selective separation, and by removing water from the sample.

Fig. 8 shows the DP distribution of the residue and the six precipitate fractions isolated from a single 400 ml sample produced under the optimal conditions for WI-LMWC (370 °C, 0.4 s). The fractions were obtained by filtration at various time intervals over a 0.45 μm membrane, as well as after partial evaporation of the sample under atmospheric pressure. In addition, Table 3 summarises the average DP values of the precipitated WI-LMWC fractions. The MWD of the samples precipitated from 45 min to 72 hours after treatment show that during the natural precipitation of the WI-LMWC the longer cellulose chains tend to precipitate first over time. The initial precipitate fraction had a DP_w of 24 while the last fraction had a DP_w of only 17. The PDI also decreased slightly, reaching values as low as 1.5, unusually low polydispersity for a cellulose sample.

In addition, evaporating water from the sample increased the apparent concentration of the oligomers dissolved in the samples, thus causing the initially soluble LMWC to precipitate additionally even after the initial precipitation of WI-LMWC was complete. Although the SEC calibration method with pullulan samples does not allow one to draw any conclusions regarding the absolute DP of the precipitated chains, the curves 6 and 7 in Fig. 8 clearly show that the last two precipitate fractions were composed of extremely low DP cellulose. The DP_w for these samples corresponding to 50% and 90% evaporation was as low as 14 and 12, respectively. These observations clearly confirm that using the differential solubility between nearcritical and ambient water enables producing narrowly distributed LMWC from MCC with no need to use any reagent other than pure water. This is especially interesting for applications involving mixtures of LMWC, as obtaining narrow DP distributions should allow a better control over the properties of the final material.

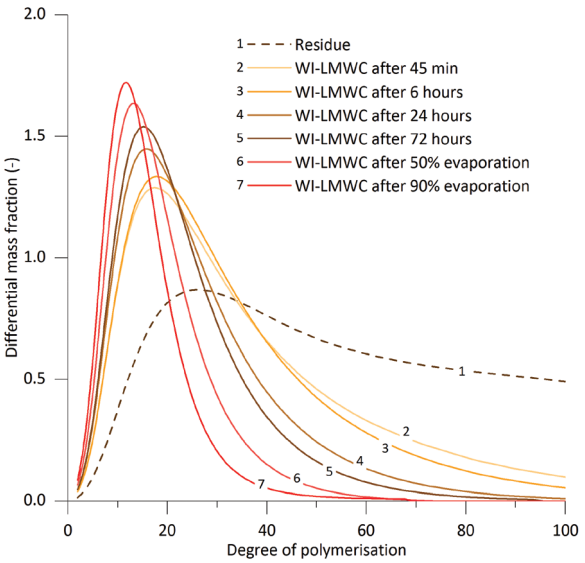

Fig. 8 Residue (curve 1), four WI-LMWC precipitate fractions (curves 2–5) recovered at various time intervals, and two WI-LMWC precipitate fractions (curves 6–7) recovered after partial evaporation of the liquid fraction, all obtained from the same 400 ml sample after treatment at 370 °C and 0.4 s.

Table 3 Number-average (DP_n), weight-average (DP_w), peak height (DP_p) degrees of polymerisation and polydispersity index (PDI) of the precipitated fractions. $DP_{50\%}$ and $DP_{90\%}$ designate the DP range given by the SEC containing 50% and 90% of the mass fraction of the samples, respectively

	DP_n	DP_w	DP_p	PDI	$DP_{50\%}$	$DP_{90\%}$
WI-LMWC after 45 min	13	24	17	1.8	11–29	5–66
WI-LMWC after 6 hours	13	22	18	1.8	11–29	5–59
WI-LMWC after 24 hours	11	18	16	1.6	10–24	5–46
WI-LMWC after 72 hours	11	17	15	1.5	10–22	5–41
WI-LMWC, 50% evaporation	9	14	13	1.5	9–19	4–32
WI-LMWC, 90% evaporation	8	12	12	1.5	8–16	4–26

4. Conclusions

In conclusion, the results presented in this work show that the nearcritical or supercritical water treatment is a versatile process able to efficiently depolymerise MCC in a controlled way. However, the intensity of the treatment must be carefully controlled in order to achieve partial cellulose depolymerisation and limit the formation of non-cellulosic products. This process allows one to obtain relatively high yields of LMWC, which is not currently available commercially, in the form of both WI-LMWC and WS-LMWC. Indeed, this hydrolysis pathway is accompanied by a phenomenon of differential solubility that can easily be leveraged to refine the final DP range of the precipitated cellulose. The fractions obtained using this technique were composed of highly crystalline cellulose II, low polydispersity, and DP_w values ranging between 12 and 24.

This work also emphasised the fact that although optimal conditions that minimise the energy demand could be identified, the high reactivity of cellulose and its hydrolysis products in nearcritical or supercritical water required a total control over the two main operating parameters: temperature, and reaction time. With several thousands of kJ per gram of product the energy demand associated with the process is high but could be greatly reduced in two ways: by selecting a more reactive cellulose than commercial MCC as a raw material, and by implementing a standard heat recovery strategy.

In any case, this hydrothermal pathway has one undeniable advantage over other depolymerisation methods: the WI-LMWC and WS-LMWC fractions can be produced with no specific inputs other than cellulose, pure water, and heat. In addition, the fractions could be isolated by simple separation methods, such as filtration and evaporation. This simplicity

makes the industrial integration of a SWCT-based LMWC plant all the more relevant in a sustainable, environmentally friendly environment.

Acknowledgements

This project was funded by Aalto University's Doctoral Programme in Chemical Technology. The authors would like to thank Rita Hatakka and Myrtel Kåll for their support with the analytical methods, as well as Lasse Tolonen for his contribution in the design of experiments.

Notes and references

1 D. Klemm, B. Heublein, H. P. Fink and A. Bohn, *Angew. Chem., Int. Ed.*, 2005, **44**, 3358–3393.
2 M. J. Taherzadeh and K. Karimi, *BioResources*, 2007, **2**, 472–499.
3 J. J. Bozell, L. Moens, D. C. Elliott, Y. Wang, G. G. Neuenscwander, S. W. Fitzpatrick, R. J. Bilski, J. L. Jarnefeld, P. Northwest, P. O. Box and K. Msin, *Resour., Conserv. Recycl.*, 2000, **28**, 227–239.
4 J. P. Lange, E. Van Der Heide, J. Van Buijtenen and R. Price, *ChemSusChem*, 2012, **5**, 150–166.
5 B. B. Hallac and A. J. Ragauskas, *Biofuels, Bioprod. Biorefin.*, 2012, 215–225.
6 M. Borrega, L. K. Tolonen, F. Bardot, L. Testova and H. Sixta, *Bioresour. Technol.*, 2013, **135**, 665–671.
7 Y. Nishiyama, P. Langan and H. Chanzy, *J. Am. Chem. Soc.*, 2002, **124**, 9074–9082.
8 C. Somerville, *Annu. Rev. Cell Dev. Biol.*, 2006, **22**, 53–78.
9 K. M. Vanhatalo and O. P. Dahl, *BioResources*, 2014, **9**, 4729–4740.
10 M. Sasaki, B. Kabyemela, R. Malaluan, S. Hirose, N. Takeda, T. Adschiri and K. Arai, *J. Supercrit. Fluids*, 1998, **13**, 261–268.
11 E. W. Lemmon, M. O. McLinden and D. G. Friend, in *NIST Chemistry WebBook, NIST Standard Reference Database Number 69*, ed. P. J. Linstrom and W. G. Mallard, National Institute of Standards and Technology, 2005.
12 A. V. Bandura and S. N. Lvov, *J. Phys. Chem. Ref. Data*, 2006, **35**, 15–30.
13 L. K. Tolonen, P. A. Penttilä, R. Serimaa and H. Sixta, *Cellulose*, 2015, **22**, 1715–1728.
14 M. Sasaki, T. Adschiri and K. Arai, *AIChE J.*, 2004, **50**, 192–202.
15 D. A. Cantero, M. Dolores Bermejo and M. José Cocero, *Bioresour. Technol.*, 2013, **135**, 697–703.
16 L. K. Tolonen, P. A. Penttilä, R. Serimaa, A. Kruse and H. Sixta, *Cellulose*, 2013, **20**, 2731–2744.
17 L. K. Tolonen, M. Juvonen, K. Niemelä, A. Mikkelson, M. Tenkanen and H. Sixta, *Carbohydr. Res.*, 2015, **401**, 16–23.
18 M. Sasaki, M. Furukawa, K. Minami, T. Adschiri and K. Arai, *Ind. Eng. Chem. Res.*, 2002, **41**, 6642–6649.
19 D. A. Cantero, M. D. Bermejo and M. J. Cocero, *ChemSusChem*, 2015, **8**, 1026–1033.
20 K. Ehara and S. Saka, *Cellulose*, 2002, **9**, 301–311.
21 O. Akpinar and M. H. Penner, *J. Food, Agric. Environ.*, 2008, **6**, 55–61.
22 G. L. Miller, J. Dean and R. Blum, *Arch. Biochem. Biophys.*, 1960, **91**, 21–26.
23 A. Buleon and H. Chanzy, *J. Polym. Sci., Polym. Phys. Ed.*, 1978, **16**, 833–839.
24 M. Meiland, T. Liebert and T. Heinze, *Macromol. Mater. Eng.*, 2011, **296**, 802–809.
25 M. Benoit, A. Rodrigues, K. De Oliveira Vigier, E. Fourré, J. Barrault, J.-M. Tatibouët and F. Jérôme, *Green Chem.*, 2012, **14**, 2212.
26 T. Nishimura and F. Nakatsubo, *Carbohydr. Res.*, 1996, **294**, 53–64.
27 Y. Yu and H. Wu, *Ind. Eng. Chem. Res.*, 2009, **48**, 10682–10690.
28 M. Sasaki, T. Adschiri and K. Arai, *J. Agric. Food Chem.*, 2003, **51**, 5376–5381.
29 M. Basholli-Salihu, M. Mueller, F. M. Unger and H. Viernstein, *Food Nutr. Sci.*, 2013, **04**, 1301–1306.
30 K. Pokusaeva, M. O'Connell-Motherway, A. Zomer, J. MacSharry, G. F. Fitzgerald and D. van Sinderen, *Appl. Environ. Microbiol.*, 2011, **77**, 1681–1690.
31 M. De la Luz Reus Medina and V. Kumar, *Int. J. Pharm.*, 2007, **337**, 202–209.
32 M. De la Luz Reus Medina and V. Kumar, *Int. J. Pharm.*, 2006, **322**, 31–35.
33 L. K. Tolonen, G. Zuckerstätter, P. A. Penttilä, W. Milacher, W. Habicht, R. Serimaa, A. Kruse and H. Sixta, *Biomacromolecules*, 2011, **12**, 2544–2551.
34 P. Ahvenainen, I. Kontro and K. Svedström, *Cellulose*, 2016, **23**, 1073–1086.
35 P. Langan, N. Sukumar, Y. Nishiyama and H. Chanzy, *Cellulose*, 2005, **12**, 551–562.
36 S. Andersson, R. Serimaa, T. Paakkari, P. Saranpaa and E. Pesonen, *J. Wood Sci.*, 2003, **49**, 531–537.
37 D. A. Cantero, M. D. Bermejo and M. J. Cocero, *J. Supercrit. Fluids*, 2013, **75**, 48–57.
38 A. Sharples, *Trans. Faraday Soc.*, 1957, **53**, 1003–1013.
39 K. B. Olanrewaju, *Reaction kinetics of cellulose hydrolysis in subcritical and supercritical water*, University of Iowa, 2012.
40 M. C. Gray, A. O. Converse and C. E. Wyman, *Appl. Biochem. Biotechnol.*, 2003, **105**, 179–193.
41 R. H. Newman, *Cellulose*, 2008, **15**, 769–778.